

## Supplementary Data

Text S1 A theoretical model for validation of the exhaustive search in MAR .....	2
Table S1 Comparison of performance of the two-step evolutionary method with other methods .....	3
Table S2 Effect of the number of search parameters on selection of potentially influential parameters.....	4
Figure S1 Convergence of parameter solutions by the two-step method in a theoretical model.....	5
Figure S2 A sensitivity distribution of two kinetic parameters in a theoretical model.....	6
Figure S3 Dynamic features for the interlocked feedback model .....	7
Figure S4 Characterization of oscillatory features for PER, dCLK, and TIM .....	8
Figure S5 Effect of the number of search parameters on separation of potentially influential parameters.....	9
Figure S6 Relationship between the CVs of period and amplitude.....	10
Figure S7 Distributions of period sensitivities and their associated kinetic parameter values.....	11
Figure S8 Distributions of amplitude sensitivities and their associated kinetic parameter values .....	12
Figure S9 Consistency of the critical parameters responsible for determining period or amplitude.....	13

### Text S1 A theoretical model for validation of the exhaustive search in MAR

To demonstrate the validity of the exhaustive search of MAR, we present a theoretical model with an autogeneous negative feedback model:

$$\frac{dy}{dt} = k \frac{K}{K + y} - y, \quad (\text{S1})$$

where  $y$  is the protein concentration,  $k$  the synthesis rate constant and  $K$  the binding constant. The protein suppresses the synthesis of itself. The steady-state concentration  $y_s$  is analytically provided by:

$$y_s = \frac{-K + \sqrt{K^2 + 4kK}}{2}. \quad (\text{S2})$$

The logarithmic gain of the steady-state concentration with respect to a kinetic parameter (sensitivity) is analytically solved and the range of the sensitivity is provided by:

$$0 < \left. \frac{\partial \ln y}{\partial \ln K} \right|_{y=y_s} < 0.5, \quad 0.5 < \left. \frac{\partial \ln y}{\partial \ln k} \right|_{y=y_s} < 1. \quad (\text{S3})$$

The target behavior is set to a steady-state concentration  $y_s$  of 1. The fitness function that the two-dimensional parameters ( $k, K$ ) must satisfy is defined by:

$$F = -|y_s - 1|. \quad (\text{S4})$$

The fitness value is constrained by:

$$|F| < \varepsilon. \quad (\text{S5})$$

where  $\varepsilon$  is the allowable error.

The kinetic parameters of the theoretical model of **Equation S1** are optimized by various evolutionary methods and a random search. Two kinetic parameters ( $k, K$ ) are explored in logarithmic space, where the basis parameter vector is set to  $(k, K) = (2, 1)$  that provides one to the steady state concentration of  $y_s$  and the allowable error is set to 0.0001. The fitness function of **Equation S4** is employed with an allowable error of **Equation S5**. In the random search (control), the value of each basis parameter was  $10^{-2}$  to  $10^2$ -fold varied randomly in logarithmic space. In the two-step search, a random search was first performed to obtain the coarse solutions with an allowable error of 0.1. Subsequently GA grew up the coarse solutions independently. The coarse solution was set to the basis parameters and the value of each basis parameter was  $10^{-1}$  to 10-fold varied randomly for the initial population for the GA. The population number was 10 and the generation number of 10. The Unimodal Normal Distribution Crossover (UNDX) was employed as the crossover method. Five elites were selected for each generation. The other evolutionary searches (UNDX, UNDXm, BLX, and SPX) employed the same logarithmic space as by the random search, where the population number was 10 and the generation number of 10. Mutation was not employed so that GAs intensively searched the neighborhood of the coarse solution.

**Table S1 Comparison of performance of the two-step evolutionary method with other methods**

Allowable error was 0.0001. The search performance was characterized by the calculation repetition number, and the mean and CV of the solution distributions. The random search was employed as a control method.

	Repetition number	mean( <i>k</i> )	mean( <i>K</i> )	CV( <i>k</i> )	CV( <i>K</i> )
<b>RS (control)</b>	<b>30300</b>	<b>16.9</b>	<b>4.00</b>	<b>1.35</b>	<b>2.75</b>
<b>Two-step</b>	<b>1700</b>	<b>16.9</b>	<b>4.01</b>	<b>1.35</b>	<b>2.89</b>
SPX	10300	12.9	4.20	1.61	2.98
UNDXm	7800	10.3	4.15	1.84	2.80
UNDX	1200	6.49	0.910	1.07	1.52
BLX	1100	7.62	7.33	1.81	2.16

For a search speed, the average repetition number of simulations that was required to find one solution was defined. The repetition number was calculated by the number of simulations being divided by the number of solutions. For the distribution of the optimized solutions, the mean and coefficient of variance (CV) of them were calculated. The mean and CV were calculated for the kinetic parameters (*k*, *K*) of **Equation S1**. A large value of CV reflects that the solutions disperse. The mean and CV of the solution distribution by the two-step search was most close to those by random search (RS), indicating that the proposed two-step method searches a given space without falling into local points, i.e., without little biases, as well as RS. SPX and UNDXm provided a larger repetition number than the two-step search. SPX and UNDXm were poor methods in terms of a calculation speed. The repetition numbers by UNDX and BLX were smaller than that by the two-step search, while the mean and CV of them are far different from those of RS. In terms of non-biased search, the two-step search was better than UNDX and BLX.

The repetition number of random searches is suggested to be important for non-biased search, because the total number of random searches carried out by the two-step method is larger than those of the UNDX and BLX methods. The solution distributions by such ordinary GA algorithms are biased compared with a random search with an increase in a calculation speed. A rapid optimization may increase the probability that a chromosome population falls into local minimums. In the two-step method, the extensive random search leads to non-biased search and the subsequent GA enables a rapid optimization.

**Table S2 Effect of the number of search parameters on selection of potentially influential parameters**

The table derives from **Figure S5**, where details in the simulation method are described. Application of a threshold value of  $10^{-8}$  to the amplitude sensitivities separates the potentially influential parameters (**Equation 10**), as marked in boldface. The kinetic parameters are sorted according to the minimum sensitivities in the descending order. The numbers of search parameters are 3 (A), 6 (B), 9 (C), 12 (D), 16 (E), 25 (F), and 36 (F), respectively. For a search parameter number of  $\geq 12$ , the members of the seventeen potentially influential parameters are the same.

<b>A</b>																	<b>3</b>																		
<b>R[1]</b>	<b>D[7]</b>	<b>A[2]</b>	<b>T[1]</b>	<b>K[2]</b>	<b>D[4]</b>	<b>R[3]</b>	<b>T[3]</b>	<b>D[10]</b>	<b>D[9]</b>	<b>D[11]</b>	<b>S[4]</b>	<b>S[3]</b>	<b>A[3]</b>	<b>D[1]</b>	<b>R[2]</b>	<b>V[2]</b>	<b>P[1]</b>	<b>D[8]</b>	<b>V[3]</b>	<b>D[3]</b>	<b>D[6]</b>	<b>S[5]</b>	<b>S[6]</b>	<b>D[2]</b>	<b>V[4]</b>	<b>A[1]</b>	<b>V[1]</b>	<b>S[2]</b>	<b>S[1]</b>	<b>D[5]</b>	<b>K[1]</b>	<b>K[4]</b>	<b>B[3]</b>	<b>B[2]</b>	<b>B[1]</b>
<b>B</b>																	<b>6</b>																		
<b>K[2]</b>	<b>D[7]</b>	<b>D[1]</b>	<b>T[1]</b>	<b>P[1]</b>	<b>D[2]</b>	<b>R[1]</b>	<b>D[3]</b>	<b>V[2]</b>	<b>S[2]</b>	<b>S[1]</b>	<b>S[3]</b>	<b>S[4]</b>	<b>R[2]</b>	<b>D[6]</b>	<b>D[4]</b>	<b>D[5]</b>	<b>K[1]</b>	<b>V[1]</b>	<b>R[3]</b>	<b>T[3]</b>	<b>D[9]</b>	<b>D[10]</b>	<b>A[2]</b>	<b>D[11]</b>	<b>A[3]</b>	<b>V[3]</b>	<b>D[8]</b>	<b>S[5]</b>	<b>S[6]</b>	<b>K[4]</b>	<b>A[1]</b>	<b>V[4]</b>	<b>B[1]</b>	<b>B[2]</b>	<b>B[3]</b>
<b>C</b>																	<b>9</b>																		
<b>D[7]</b>	<b>K[2]</b>	<b>S[4]</b>	<b>S[3]</b>	<b>R[1]</b>	<b>T[1]</b>	<b>D[3]</b>	<b>D[5]</b>	<b>P[1]</b>	<b>R[2]</b>	<b>D[6]</b>	<b>D[1]</b>	<b>D[2]</b>	<b>K[1]</b>	<b>S[1]</b>	<b>S[2]</b>	<b>D[4]</b>	<b>V[2]</b>	<b>V[1]</b>	<b>S[5]</b>	<b>S[6]</b>	<b>A[1]</b>	<b>A[2]</b>	<b>A[3]</b>	<b>R[3]</b>	<b>B[1]</b>	<b>B[2]</b>	<b>B[3]</b>	<b>V[3]</b>	<b>V[4]</b>	<b>D[8]</b>	<b>D[9]</b>	<b>D[10]</b>	<b>D[11]</b>	<b>T[3]</b>	<b>K[4]</b>
<b>D</b>																	<b>12</b>																		
<b>D[1]</b>	<b>T[1]</b>	<b>D[4]</b>	<b>D[3]</b>	<b>S[3]</b>	<b>S[4]</b>	<b>D[5]</b>	<b>P[1]</b>	<b>D[7]</b>	<b>S[1]</b>	<b>S[2]</b>	<b>V[1]</b>	<b>K[1]</b>	<b>D[6]</b>	<b>V[2]</b>	<b>D[2]</b>	<b>K[2]</b>	<b>R[3]</b>	<b>T[3]</b>	<b>D[9]</b>	<b>D[10]</b>	<b>A[2]</b>	<b>A[1]</b>	<b>D[8]</b>	<b>D[11]</b>	<b>S[6]</b>	<b>S[5]</b>	<b>A[3]</b>	<b>R[1]</b>	<b>R[2]</b>	<b>B[1]</b>	<b>B[2]</b>	<b>B[3]</b>	<b>V[3]</b>	<b>V[4]</b>	<b>K[4]</b>
<b>E</b>																	<b>16</b>																		
<b>S[1]</b>	<b>S[2]</b>	<b>D[1]</b>	<b>K[1]</b>	<b>D[4]</b>	<b>D[3]</b>	<b>P[1]</b>	<b>S[3]</b>	<b>S[4]</b>	<b>D[2]</b>	<b>D[6]</b>	<b>D[5]</b>	<b>T[1]</b>	<b>V[1]</b>	<b>D[7]</b>	<b>V[2]</b>	<b>K[2]</b>	<b>R[3]</b>	<b>K[4]</b>	<b>S[6]</b>	<b>A[3]</b>	<b>D[11]</b>	<b>V[3]</b>	<b>T[3]</b>	<b>A[1]</b>	<b>D[9]</b>	<b>D[10]</b>	<b>S[5]</b>	<b>A[2]</b>	<b>R[1]</b>	<b>R[2]</b>	<b>B[1]</b>	<b>B[2]</b>	<b>B[3]</b>	<b>V[4]</b>	<b>D[8]</b>
<b>F</b>																	<b>25</b>																		
<b>D[4]</b>	<b>T[1]</b>	<b>K[2]</b>	<b>P[1]</b>	<b>D[7]</b>	<b>S[3]</b>	<b>K[1]</b>	<b>D[1]</b>	<b>D[2]</b>	<b>S[2]</b>	<b>V[1]</b>	<b>D[3]</b>	<b>D[6]</b>	<b>V[2]</b>	<b>S[1]</b>	<b>D[5]</b>	<b>S[4]</b>	<b>S[5]</b>	<b>S[6]</b>	<b>A[1]</b>	<b>A[2]</b>	<b>A[3]</b>	<b>R[1]</b>	<b>R[2]</b>	<b>R[3]</b>	<b>B[1]</b>	<b>B[2]</b>	<b>B[3]</b>	<b>V[3]</b>	<b>V[4]</b>	<b>D[8]</b>	<b>D[9]</b>	<b>D[10]</b>	<b>D[11]</b>	<b>T[3]</b>	<b>K[4]</b>
<b>G</b>																	<b>36</b>																		
<b>D[1]</b>	<b>D[3]</b>	<b>K[1]</b>	<b>S[2]</b>	<b>P[1]</b>	<b>S[1]</b>	<b>D[4]</b>	<b>S[3]</b>	<b>S[4]</b>	<b>D[5]</b>	<b>V[1]</b>	<b>D[7]</b>	<b>T[1]</b>	<b>D[2]</b>	<b>K[2]</b>	<b>D[6]</b>	<b>V[2]</b>	<b>S[5]</b>	<b>S[6]</b>	<b>A[1]</b>	<b>A[2]</b>	<b>A[3]</b>	<b>R[1]</b>	<b>R[2]</b>	<b>R[3]</b>	<b>B[1]</b>	<b>B[2]</b>	<b>B[3]</b>	<b>V[3]</b>	<b>V[4]</b>	<b>D[8]</b>	<b>D[9]</b>	<b>D[10]</b>	<b>D[11]</b>	<b>T[3]</b>	<b>K[4]</b>

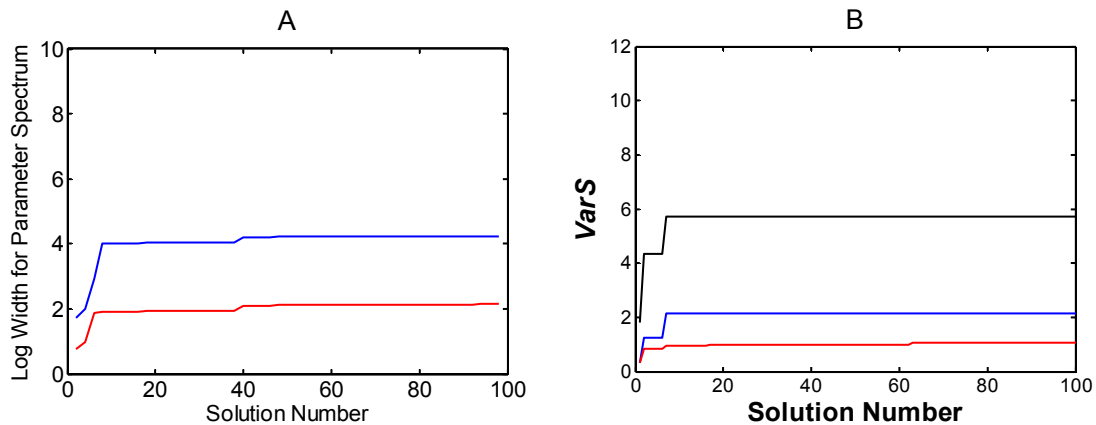


**Figure S1 Convergence of parameter solutions by the two-step method in a theoretical model**

(A) Convergence of the logarithmic width of the parameter spectrum for two parameters. One hundred of solutions for optimized kinetic parameters were obtained by using the repetition of the two-step search. The blue line is  $K$  and the red line  $k$ . (**Equation S1**)

(B) Convergence for the variability in the solutions of kinetic parameters. Three clusters were generated from using the early 40 solutions. The number of the employed clusters is changed from 1 to 3.  $VarS$  (**Equation 7**) is plotted with respect to the solution number.  $VarS$  of less than one shows that the generated solutions are included in the employed clusters. The black line is one cluster employed, the blue line two clusters, and the red line three clusters.

The parameter spectrum width spreads with an increase in the solution number, indicating that the variability in the solution vectors becomes large. The spectrum width is almost saturated above 40 (**Figure S1A**). A hierarchical clustering with the average linkage method is applied to the initial 40 solutions, classifying the solution vectors into three clusters. By using three clusters, we investigate the convergence for the  $VarS$  value as shown in **Figure S1B**. The  $VarS$  value decreases with an increase in the number of the employed clusters. When all the three clusters are used, the  $VarS$  value begins to converge close to one at 40. The two-step method approaches saturation or covers almost the entire solution space at a solution number of 40 in the given search parameter space.

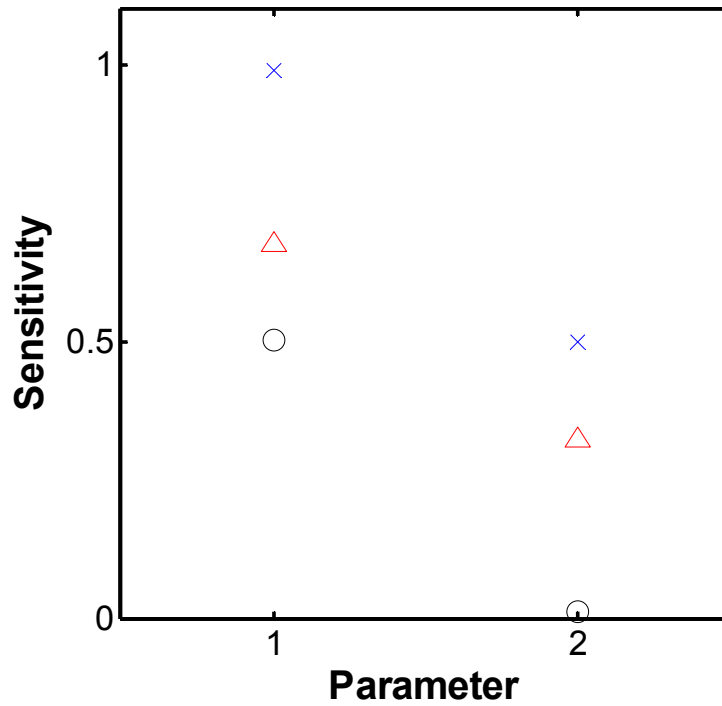


**Figure S2 A sensitivity distribution of two kinetic parameters in a theoretical model**

The sensitivity distributions were numerically calculated by changing each kinetic parameter by one percentage. Forty solutions are employed. The mean (red triangle), minimum (black circle), and maximum (blue cross) values are plotted with respect to each kinetic parameter. 1 is  $k$  and 2 is  $K$ .

The range of the simulated sensitivity is consistent with the theoretical range (**Equation S3**), showing that MAR predicts the sensitivity range precisely. The sensitivity for  $k$  cannot be suppressed to be less than 0.5, whereas that for  $K$  can be reduced to zero. When the threshold value is set to 0.5, the parameter of  $k$  is the potentially influential parameter responsible for the steady-state level.

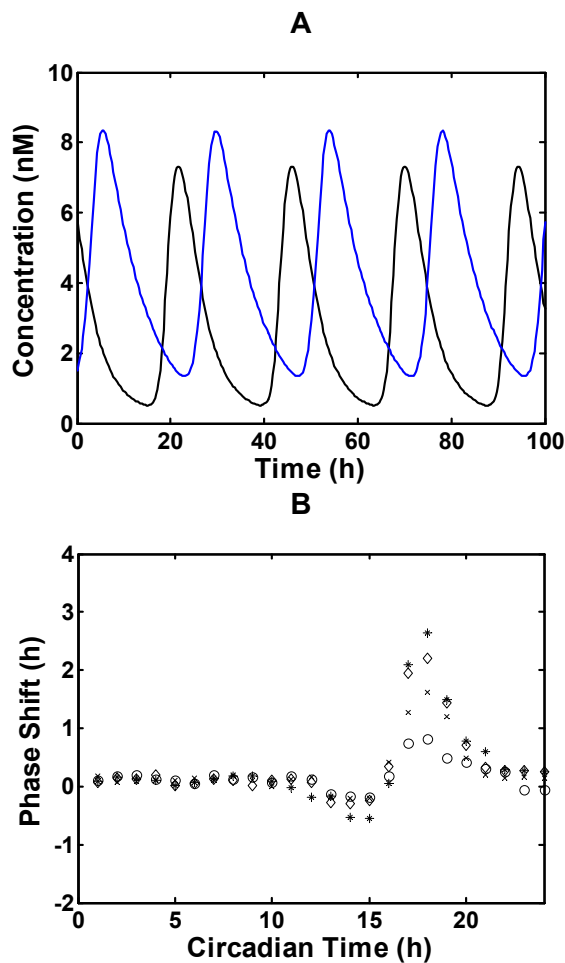


### Figure S3 Dynamic features for the interlocked feedback model

(A) Time evolution for the total concentrations for PER and dCLK. The black curve is PER and the blue curve is dCLK. The model reproduces the typical experimental features that the time evolutions for PER and dCLK oscillate in turn. There are few experimental data regarding the absolute concentration of the circadian proteins. The simulated time courses of the proteins are consistent with those presented by commonly used mathematical models, e.g., the PER and dCLK concentrations vary from a few nM to a few dozen nM [1].

(B) Light pulse-induced phase shift of the peak time for mRNA for PER. Since TIM is degraded by light, we emulate light pulse by increasing the degradation rate constant ( $D[5]$ ) for TIM by 2- (open circle), 4- (cross), 8- (diamond), or 16-fold (star) for 1 h. We apply the same promotion of TIM degradation to the model on 24 different circadian time points and measure the following peak time of *per* mRNA. By comparing it with the peak time of *per* mRNA without perturbation, we calculate the phase shifts.

The phase shifts occurs depending on the circadian time at which perturbation is applied. The simulated results are consistent with the observation that light-pulses delay the phase of the circadian activity rhythms during early subjective night and advance the phase during late subjective night whereas light pulses tend to cause minimal or no phase shifts during the subjective day [2], although the simulated phase delay at 15 h is smaller than the experimental observation.

### References

1. Smolen P, Baxter DA, Byrne JH (2001) Modeling circadian oscillations with interlocking positive and negative feedback loops. *J Neurosci* 21: 6644-6656.
2. Hall JC, Rosbash M (1987) Genes and biological rhythms. *Trends Genet* 3: 185-191.

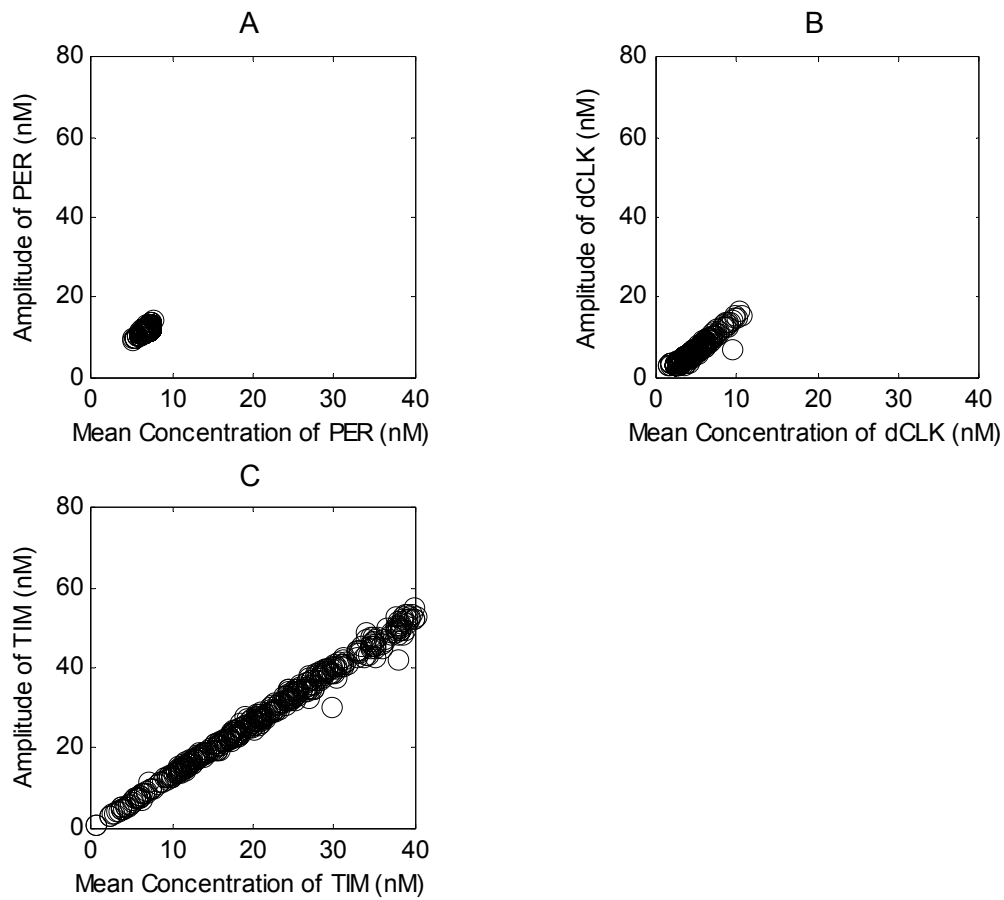


**Figure S4 Characterization of oscillatory features for PER, dCLK, and TIM**

We investigate the cycle features of PER, dCLK and TIM when the circadian model is optimized with regard to the PER oscillator. The amplitudes and the mean concentrations of PER (A), dCLK (B), and TIM (C) are plotted.

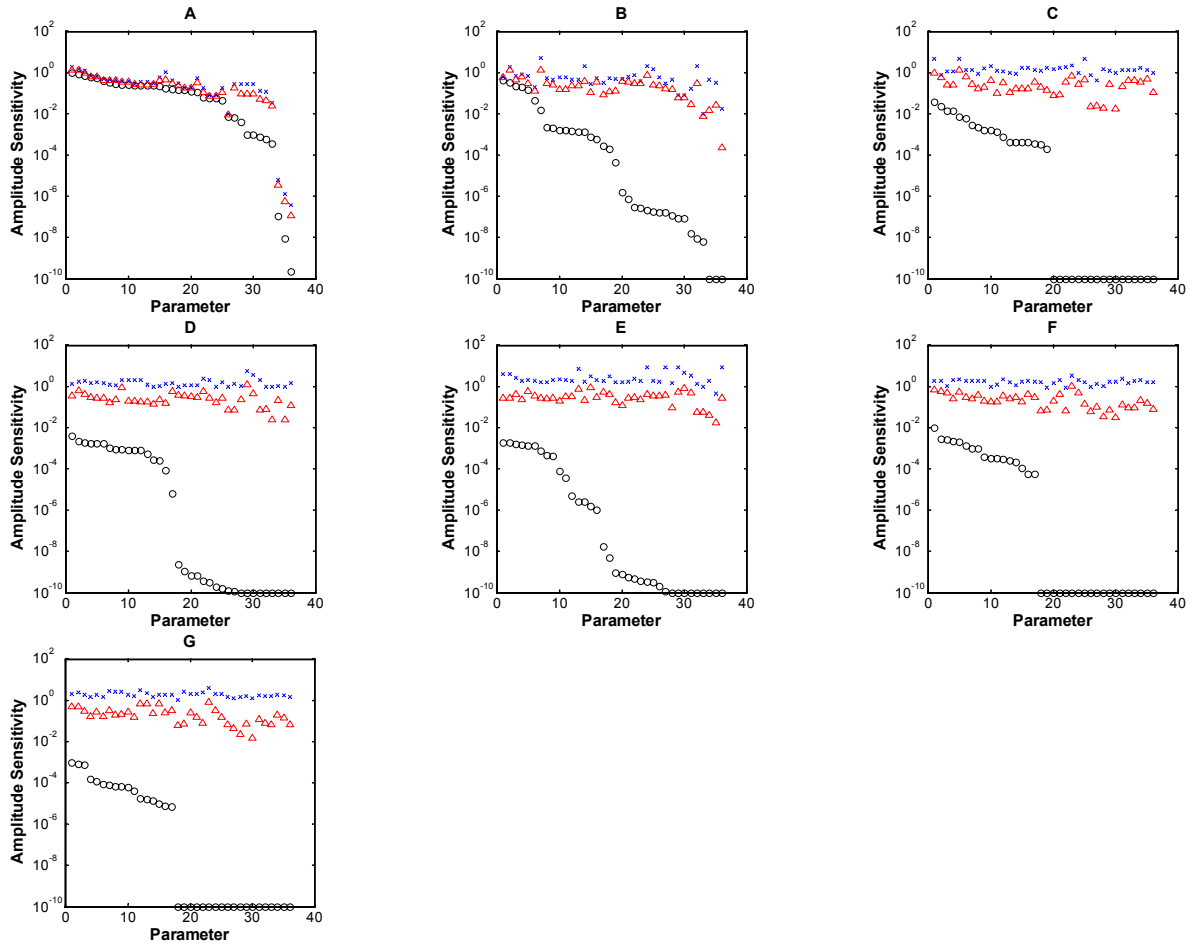


**Figure S5 Effect of the number of search parameters on separation of potentially influential parameters**

We investigated how the number of search parameters distinguishes the potentially influential parameters (**Equation 10**). For various numbers of search parameters, we generated 400 solutions optimized for a PER cycle and then simulated the absolute value of the amplitude sensitivity when each kinetic parameter was varied by 2-fold. The resulting distributions exclude the models whose oscillations are abolished by parameter perturbations ( $|Sensitivity| > 10$ ). The amplitude sensitivities with a value of less than  $10^{-10}$  are set to  $10^{-10}$ .

The kinetic parameters are sorted according to the minimum sensitivity (black circle) in the descending order. The mean value (red triangle) and the maximum sensitivity (blue cross) are also plotted. The label of the figures shows: (A) explores 3 parameters ( $S[1], A[1], A[2]$ ), (B) 6 parameters ( $S[1], A[1], A[2], R[1], R[2], V[1]$ ), (C) 9 parameters ( $S[1], A[1], A[2], R[1], R[2], V[1], V[2], D[1], P[1]$ ), (D) 12 parameters ( $S[1], A[1], A[2], R[1], R[2], V[1], V[2], D[1], P[1], T[1], K[1], K[2]$ ), (E) 16 parameters ( $S[1], A[1], A[2], R[1], R[2], V[1], V[2], D[1], P[1], T[1], K[1], K[2], S[4], D[3], D[5], D[7]$ ), (F) 25 parameters ( $S[1], A[1], A[2], R[1], R[2], V[1], V[2], D[1], P[1], T[1], K[1], K[2], S[4], D[3], D[5], D[7], S[3], A[3], R[3], V[3], V[4], D[8], D[11], T[3], K[4]$ ), (G) the entire 36 parameters.

The values of  $T[2], T[4], K[3]$ , and  $K[5]$  are set to zero.

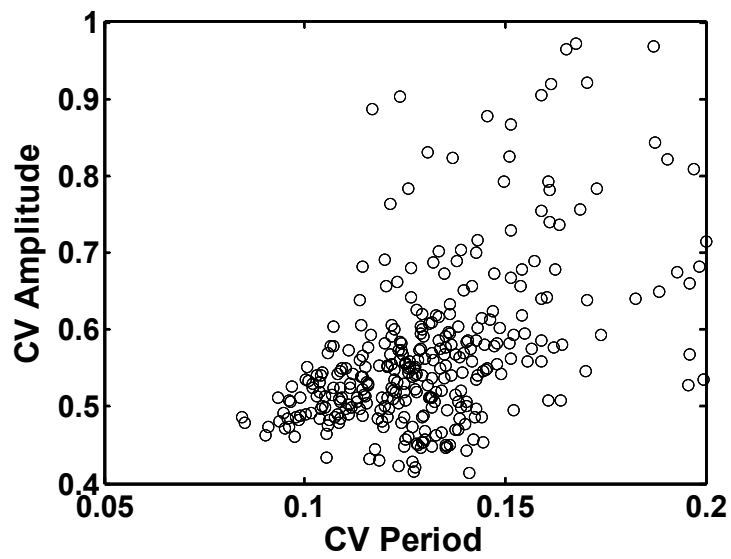


**Figure S6 Relationship between the CVs of period and amplitude**

The CVs for the period distribution generated by the random simulations are plotted with respect to the CVs for the amplitude distributions.

Significant linear correlation was not observed between the CVs of period and amplitude. The mechanism that provides a robust property to the period is suggested to be different from that to the amplitude.

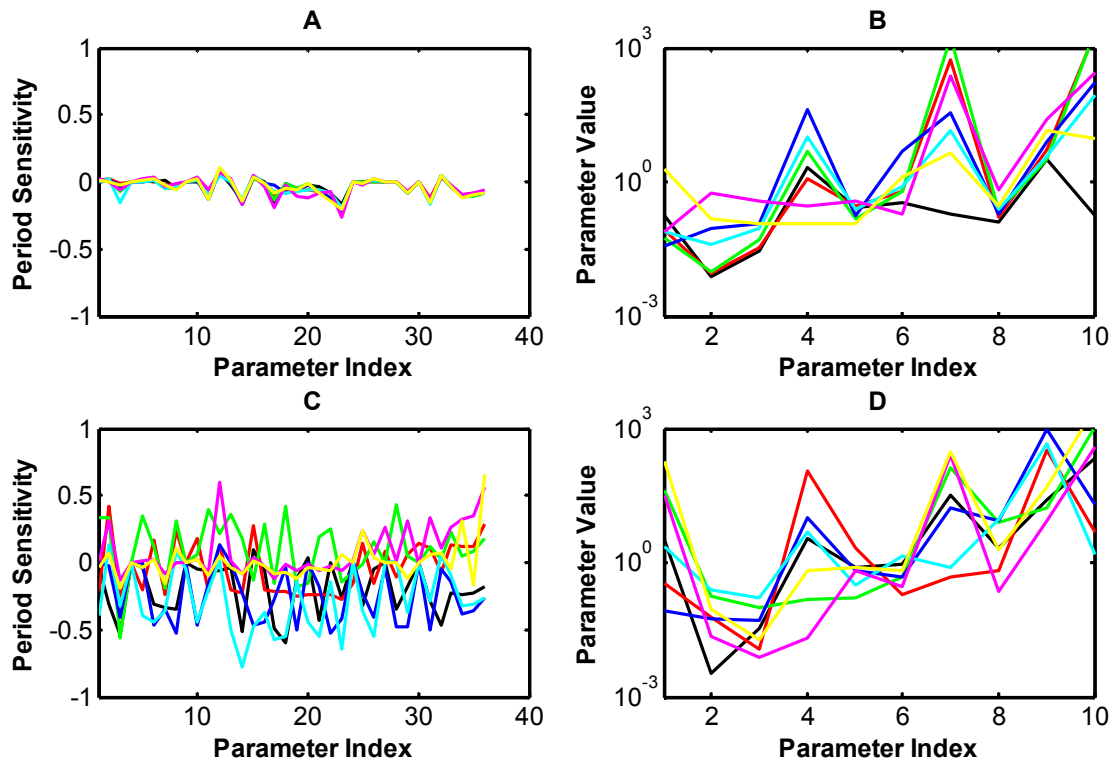


**Figure S7 Distributions of period sensitivities and their associated kinetic parameter values**

In the upper panels, the period sensitivity (A) and parameter value (B) distributions of the models showing seven smaller values of the CV period are plotted. A parameter index of one indicates  $S[1]$ , 2:  $A[1]=A[2]$ , 3:  $R[1]=R[2]$ , 4:  $V[1]$ , 5:  $V[2]$ , 6:  $D[1]$ , 7:  $P[1]$ , 8:  $T[1]$ , 9:  $K[2]$ , 10:  $K[1]$ .

In the lower panels, the amplitude sensitivity (C) and parameter value (D) distributions of the models showing seven larger values of the CV period are plotted.

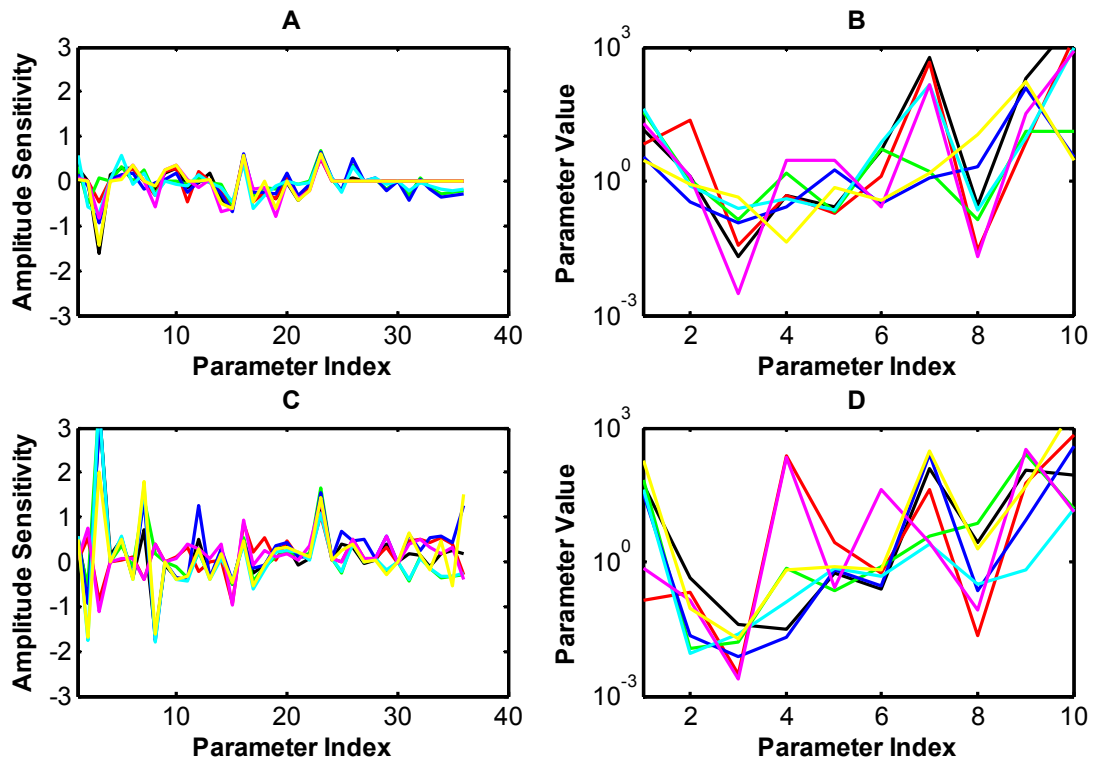


**Figure S8 Distributions of amplitude sensitivities and their associated kinetic parameter values**

In the upper panels, the amplitude sensitivity (A) and parameter value (B) distributions of the models showing seven smaller values of the CV amplitude are plotted. A parameter index of one indicates  $S[1]$ , 2:  $A[1]=A[2]$ , 3:  $R[1]=R[2]$ , 4:  $V[1]$ , 5:  $V[2]$ , 6:  $D[1]$ , 7:  $P[1]$ , 8:  $T[1]$ , 9:  $K[2]$ , 10:  $K[1]$ .

In the lower panels, the amplitude sensitivity (C) and parameter value (D) distributions of the models showing seven larger values of the CV amplitude are plotted.

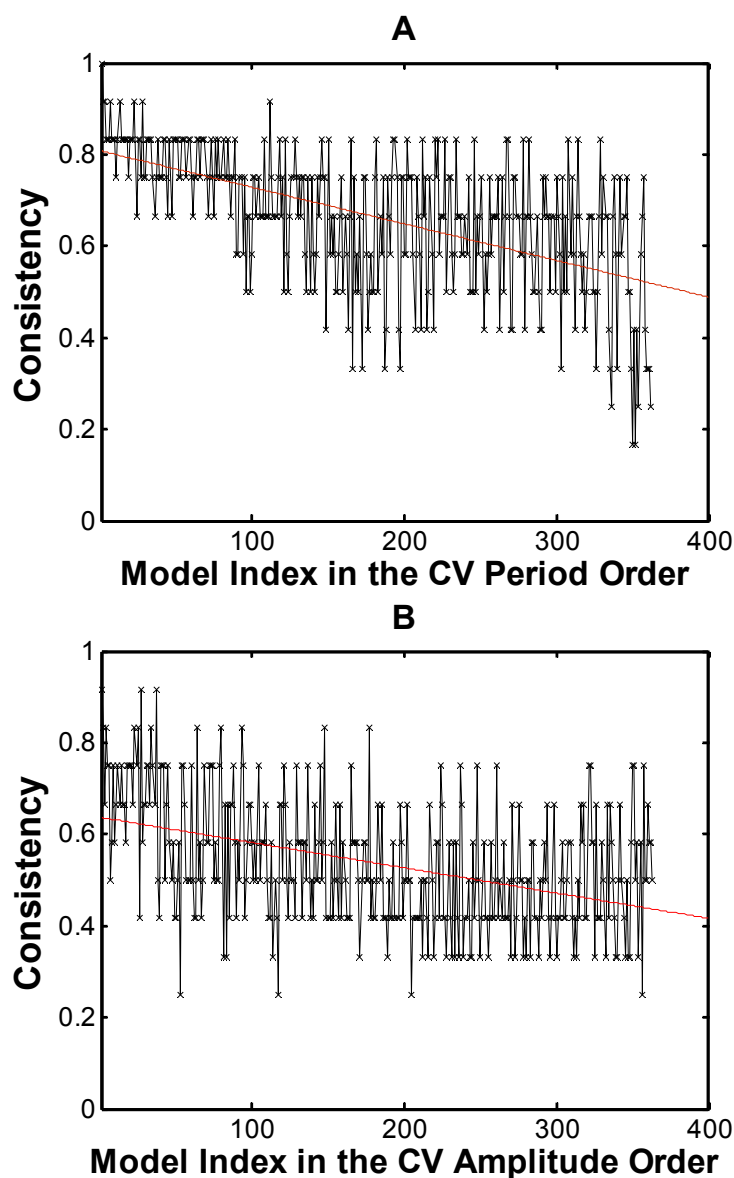


**Figure S9 Consistency of the critical parameters responsible for determining period or amplitude**

The twelve critical parameters for determining period and amplitude were selected from **Figure 9**, respectively. To investigate whether these twelve critical parameters feature robust oscillation, the consistency was defined. For each model, 12 kinetic parameters showing a higher absolute sensitivity were selected and the number of the selected kinetic parameters corresponding to the selected critical parameters was counted. The consistency is provided as the ratio of the number of the corresponding number to 12 and is plotted with respect to the models sorted in the ascending order of the CV values.

(A) Consistency of the twelve critical parameters responsible for period,

(B) Consistency of the twelve critical parameters responsible for amplitude.

With a decrease in the CV value, the consistency increases, indicating that the selected critical parameters feature highly robust models with a small CV value. The selected parameters are found significantly critical for determining period or amplitude in the highly robust models.